Laser Tracker, a handy tool for metrology and alignment

George J. Wojcik and Stuart A. Lakanen
Particle Physics Division: Alignment and Metrology Group
Fermi National Accelerator Laboratory, Batavia, Illinois

1. Abstract

The Laser Tracker is used for various survey and alignment problems at Fermilab. The authors of this paper will discusses several applications of Laser Tracker measurement successfully used by the Metrology and Alignment Group. The main concerns of this paper will deal with the efficient design of methods to provide viable data for the alignment of high energy experiments.

2. Introduction

Through different applications of measurement, the Laser Tracker is most nearly the universal tool for metrology and alignment. The Metrology and Alignment group have developed a variety of field measurement and calculation procedures that have been used through out the laboratory. The Laser Trackers were used for measurement of precise underground tunnel networks as well as measuring small objects, referencing of the magnetic components, and as-founds of beam line components.

3. Networks measurement and adjustment

The Alignment and Metrology group has performed survey of several networks including:

3.1. Antiproton tunnel networks surveyed 1995 and 2000 with the simultaneous survey as found of components.
3.2. FMI underground tunnel networks surveyed 1996 and 1998.
3.3. The CDF Collision Hall network survey of 1998.
3.4. The CDF Detector network survey 1999.
3.5. The A0 and Switchyard 2001 network survey

A view of the antiproton tunnel is shown on Picture1, while Picture 2 displays a view of the Fermilab Main Injector tunnel. The main concern of the design of the underground control networks is to meet the accuracy specifications needed to position the beam lines components and beam monitoring devices. A pre-analysis of this criteria resulted with the selection of the Laser Tracker to perform the three dimensional trilateration networks. Several networks have been measured with the Chesapeake 3000 & 4000 Laser Trackers, combined with measurements made with the Kern Mekometer ME5000, the Kern E2, the Geodimeter 640, and Leica NA3000.

The trilateration networks reported in Cartesian coordinates of the surveyed points were not in a gravity-based system. The Laser Tracker head coordinates were converted to pseudo observations – weighted slope distances. The slope distances were calculated from two or more Laser Tracker stations with weights being calculated according to the factory specification of the Laser Tracker.

Picture 1. Typical view of antiproton tunnel

Picture 2. View of FMI tunnel

Laser tracker pseudo observations were evaluated to removed gross errors by comparing redundant distances from different Laser Tracker stations with a rejection criteria based on the standard deviation of observations. Table 1 gives examples of rejected observations. If any distance was rejected, the points were reobserved.

Table 1. Examples of rejected observations

FROM	TO	STD ERR	DISTANCE	
615A_1	D6B14	0.00004	3.834845	
615A_1	D6B14	0.00005	3.834745	
615A_1	D6B14	0.00006	3.835251	
		SDEV DIS=	0.00027	REJECT.VALUE=0.00012
615A_1	PP005	0.00003	6.255444	
615A_1	PP005	0.00004	6.255716	
615A_1	PP005	0.00005	6.255960	
		SDEV DIS=	0.00028	REJECT.VALUE=0.00012

The accuracy requirement for the networks was calculated a priori to meet the required accuracy dictated by the experiment. The antiproton network required a positional accuracy of +/- 0.1 mm for both the X and Y coordinate. The Main Injector required an accuracy of +/- 0.15mm over one betatron wave length, 127.699 m. In addition,, the circumference of the tunnel was to be established to +/- 10 mm, an implied radial accuracy across the ring of +/- 2 mm. For small networks: CDF, the CDF Detector, A0 and Switchyard required accuracy falling below +/-0.1 mm. (*Accuracy of points for all networks listed is a one-sigma – probability of 63%*).
The underground networks have 4 types of monuments: floor points, wall points, pass points and points on the components. The wall monuments are automotive tie rod ends and used primarily as vertical monuments. See Picture 3

Picture 3. Vertical tunnel wall monuments with bar code scale and SMR

The old tunnel monuments are brass rods imbedded in the floor, while the new floor monuments,Dijak plugs, consist of a ¾" x 10 diameter stainless steel bolt, machined to accept a 0.250" pin for various fixtures and attachments. Connected to a ¾" x 1 diameter stainless nut, this assembly is grouted into the concrete floor. Brass rods and tunnel passpoints are shown in

Picture 4. Horizontal tunnel floor monuments, pass point, and centering plate over brass

Please refer to Picture 5, showing a model of the Dijak plug with SMR in place and Picture 6 a tunnel shot of an SMR on a Dijak plug.

Picture 5. A model of the Dijak plug

Picture 6. Tunnel monument with SMR

4. As found of components of the beam lines

Laser Trackers were used on several projects to reference magnets on the fly in the experimental beam lines to allow for the immediate alignment of the components . The alignment group measured all of the components of Antiproton Ring and 8Gev line. The strategy of measuring the components was to sufficiently map each component so that its geometry and function could be well enough determined to be able to immediately align the component to its beam line position.

The following example demonstrates the as founding and referencing of the components used by the antiproton accumulator. Components on the antiproton ring can be described as:

1. Bending magnets, or dipoles. Dipoles are like bar magnets that bend the beam direction left, right, up, or down.
2. Focusing magnets, or quadruples. Quadrapole magnets focus the beam; they exert a restoring magnetic force back toward the center.
3. Correction magnets: these adjust for imperfections of magnetic fields and alignments. They are typically dipoles in the vertical or horizontal and are referred to as “trims”. Sextuple magnets (six pole pieces) make higher-order corrections to the focusing of the beam.

Periodic surveys check the position of the components and are used to monitor the deformation of the tunnel and the geometry of the machine.

4.1. Measurement and Calculation of Dipoles

A Dipoles is shown in Picture 7.

Picture 7. Dipoles antiproton bending magnets

This dipole was mapped by scanning the top and bottom grooves in the laminations, locating the center hole as established at the magnet factory and measuring the upstream and downstream faces of the magnet. The 0.750” radius SMR does not give the lamination point directly. Each measurement has to then be corrected by transferring from the center of the spherical measuring device to the lamination. See Figure 1 for an example of the calculation correction for one of lamination grooves.

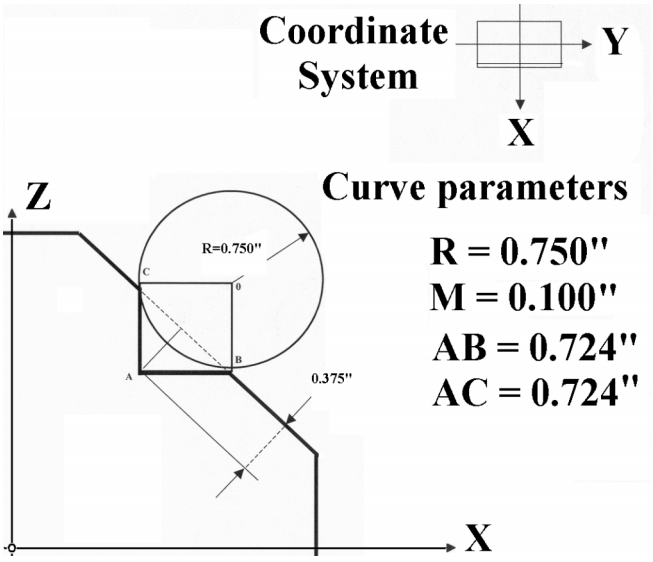

Figure 1. Calculation SMR correction

Figure 2 shows how we used the laser tracker and the array of lamination points used in the referencing.

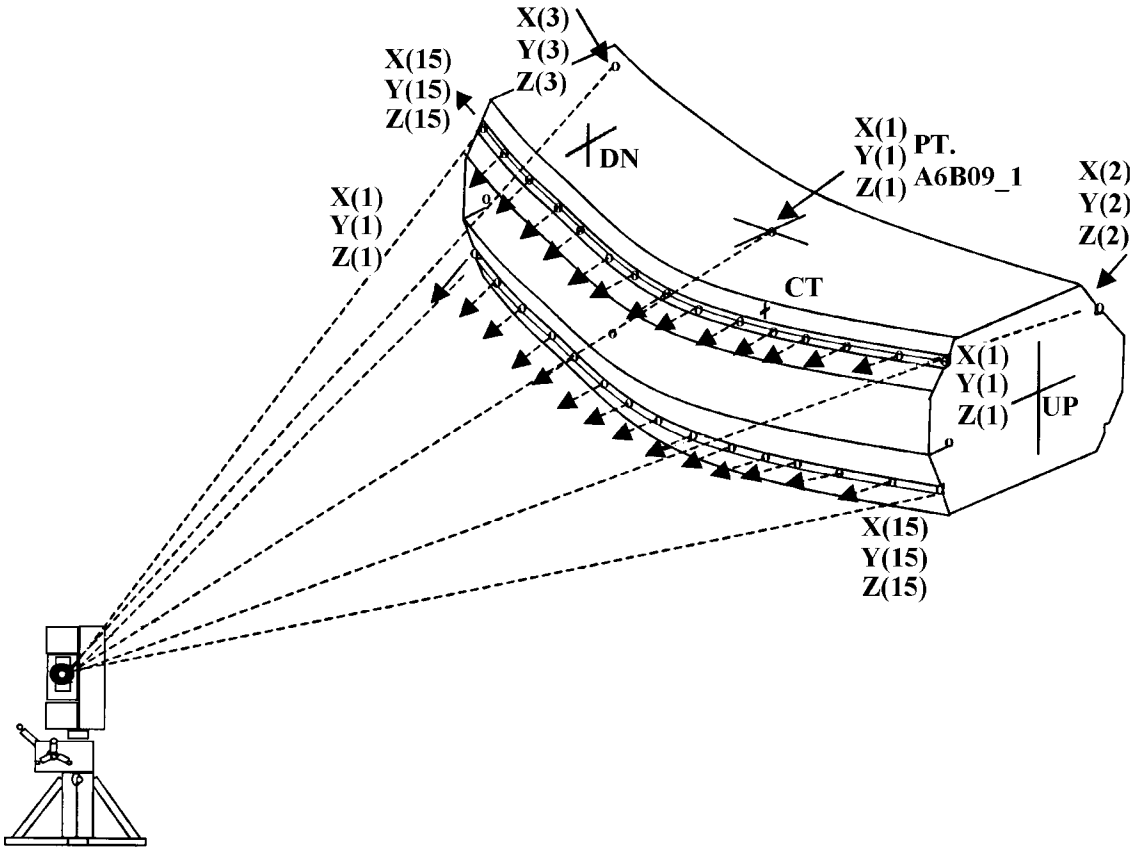

Figure 2. Laser Tracker station with schematic rays for mapping grooves

Other components have different sizes but the same shape allowing the use of the same mapping pattern. During the mapping stage the units were measured in inches to more easily relate the findings of the reference work done with optical tooling in the past. The Laser Tracker reported coordinates in a non-gravity instrument coordinate system. To calculate the position in antiproton tunnel coordinates system, field data were transformed to the antiproton coordinate system using the adjusted coordinates of the network. Transformed laser tracker observations for a dipole are shown on Table 2. The seven-parameter transformation included the three-dimensional position, the three rotation angles, and scale. More details will be shown in our quadrapole discussion in Section 4.2.

Table 2. Laser Tracker observations for dipole after transformation.

TOP	**X(inches)**	**Y(inches**	**Z(inches**
1	-2733.071	-14943.773	116.221
2	-2720.758	-14943.966	116.208
3	-2708.959	-14944.348	116.192
4	-2696.838	-14944.959	116.179
5	-2684.933	-14945.789	116.160
6	-2672.855	-14946.854	116.147
7	-2661.116	-14948.101	116.142
8	-2649.111	-14949.587	116.141
9	-2637.163	-14951.241	116.142
10	-2625.346	-14953.088	116.145
11	-2613.303	-14955.191	116.150
12	-2601.567	-14957.460	116.156
13	-2589.864	-14959.943	116.156
14	-2578.153	-14962.653	116.149
15	-2566.403	-14965.597	116.146
BOTTOM			
1	-2566.279	-14965.654	85.197
2	-2577.896	-14962.727	85.204
3	-2589.514	-14960.034	85.207
4	-2601.206	-14957.547	85.208
5	-2612.993	-14955.266	85.199
6	-2624.890	-14953.172	85.194
7	-2636.543	-14951.337	85.190
8	-2649.055	-14949.609	85.188
9	-2660.920	-14948.135	85.191
10	-2673.140	-14946.839	85.201
11	-2684.997	-14945.804	85.211
12	-2697.023	-14944.982	85.228
13	-2709.183	-14944.361	85.247
14	-2709.219	-14944.358	85.248
15	-2733.443	-14943.780	85.270
CENTER			
1	-2652.101	-14973.851	120.196
BACK			
2	-2722.156	-14991.394	119.487
3	-2575.329	-15011.878	119.462

The center of the magnet is determined by fitting the top and bottom groove data to a circle, defining $\mathbf{C_t}$, the center, as defined by the top groove; $\mathbf{C_b}$, the center defined by the bottom groove and their average, $\mathbf{C_o}$. Previously, optical tooling had been used to reference the relationship between the center hole set at the magnet factory and the electronically established magnetic center. See the Figure 12.

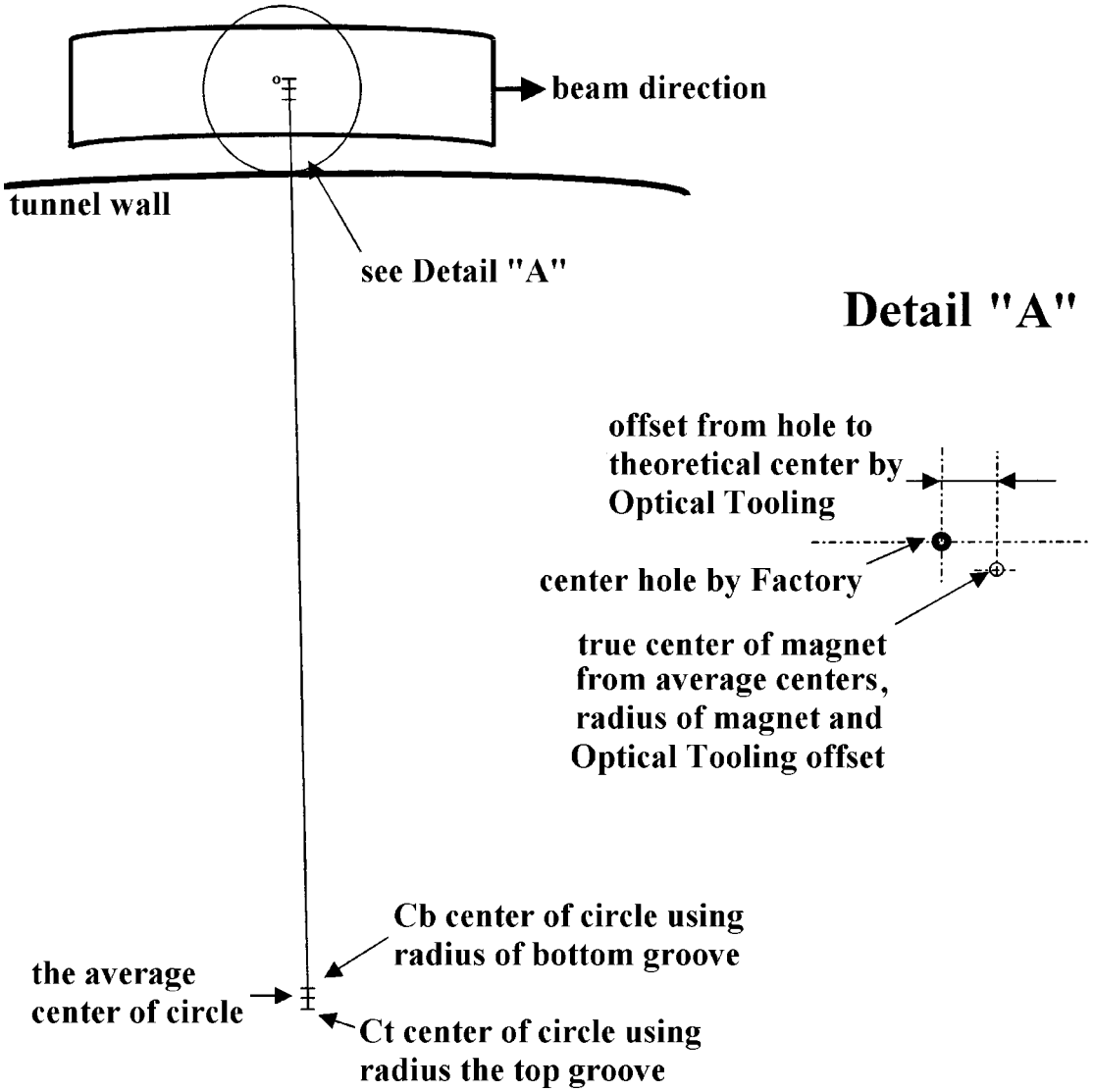

Figure 3. Sketch of dipole calculation strategy

The true center of the magnet was determined using the average center of the circle, the theoretical radius and the offset determined with optical tooling. Using the half sizes of the component, the position, roll and pitch of the magnet was determined. The data were verified against the ideal parameters of the dipole to detect measurement errors.

4.2. Measurement and Calculation of Quadrupoles

The next Picture 8 displays an antiproton quadruple focusing magnet.

Picture 8. Quads antiproton a focusing magnets

Like the dipole components, the quadruples have the same shape but different sizes, permitting the use of the same mapping pattern. This shape required 3 points on both the top and bottom grooves, the upstream and down stream points on the top back groove and 1 point on the upstream face of the quadrapole. Before the final calculation was performed the raw data were transformed to the antiproton tunnel coordinate system. Appendix A shows the results of the 7 parameter transformation as was done on the dipoles. Laser tracker transformed observations for quadrapole components are shown on Table 3.

Table 3. Laser Tracker observations for quad after transformation.

TOP	**X(inches)**	**Y(inches)**	**Z(inches)**
1	-5338.830	-16510.840	114.109
2	-5334.072	-16502.596	114.109
3	-5328.680	-16493.266	114.103
BOTTOM			
1	-5330.247	-16495.951	87.539
2	-5333.533	-16501.646	87.539
3	-5337.538	-16508.576	87.542
BACK			
1	-5329.622	-16516.919	117.446
2	-5319.457	-16499.924	117.430

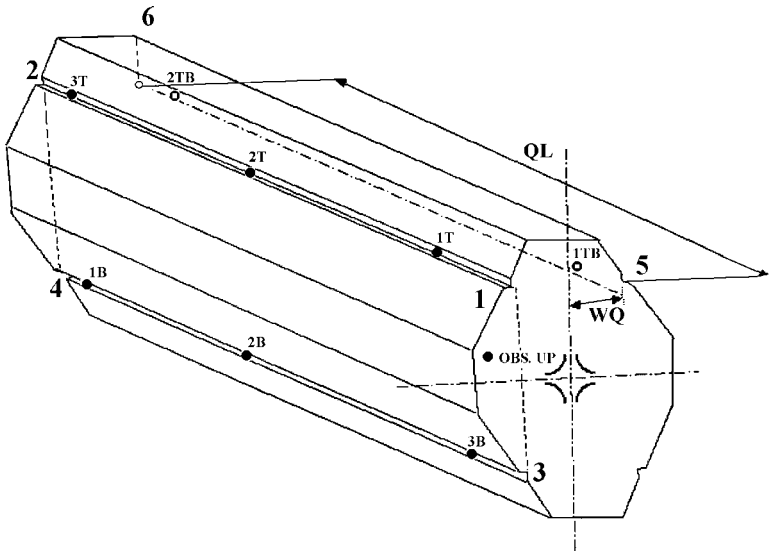

Figure 4.Sketch of antiproton quads with survey points.

Please refer to Figure 4. The top groove measurements are fit to a line and the intersection of a ninety-degree offset to the upstream face point is computed. A second ninety-degree offset is computed using the bottom grooves. Using the ideal length and the two best-fit lines the downstream end of the magnet is computed. The two best-fit lines are used to create a plane that is then compared to a gravity plane. The angle between the two planes defines the roll angle of the magnet. The pitch angle is determined by first finding the midpoints of the lines between the top and bottom grooves at the upstream and downstream ends of the magnets. Using these midpoints and the ideal distance from the groove to the centerline, the center of the magnet is computed at both ends using a ninety-degree offset. The inverse between the centers of the magnet will produce the pitch angle. The mean of the upstream and downstream centerline points will result in the midpoint of the magnet. The data was verified against the ideal parameters of the quadrapole to eliminate measurement errors.

4.3 Measuring the correction magnet

The correction magnet is simply described as being a box. See Figure 5. Three measurements were taken on the upstream face; three were taken on the top while just two points were observed on one side. The standard seven-parameter transformation was made to the antiproton coordinates system as shown in Table 4.

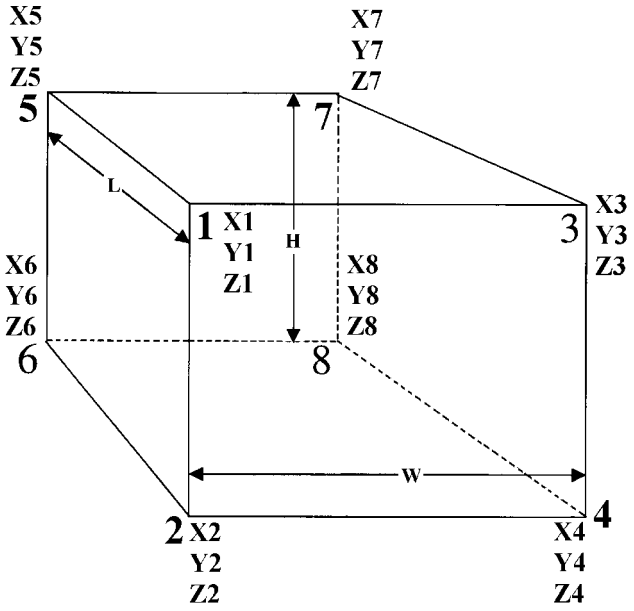

Figure 5. Sketch of antiproton trim magnet calculation strategy

A plane was computed the upstream measurements and a second plane was determined from the top values. The intersection of these two planes created a normal vector of side plane. Using this vector and a point from the side, the side plane is defined. A check is made to the second point on the side to make sure the computation is working correctly. Then using the ideal dimensions, parallel planes are created for remaining three sides. The intersections of the six planes will define the 8 corners. Mean values with corresponding intersections define the pitch angles; roll angles, the upstream and downstream ends and center. This method only works for correction magnets where accuracies need only be accurate to a few millimeters.

Table 4. Laser Tracker observations for trim magnet after transformation file.

AH105.CSV	X(inches)	Y(inches)	Z(inches)
UP			
1	-4809.151	-15714.927	113.203
2	-4811.070	-15713.559	109.745
3	-4811.092	-15713.543	95.906
TOP			
1	-4800.179	-15713.883	112.005
2	-4803.198	-15718.663	112.003
3	-4808.336	-15715.044	112.013
SIDE			
1	-4806.659	-15709.644	109.741
2	-4809.891	-15714.098	108.629

Software was developed during the antiproton project to analyze and compute data for typical parts of the antiproton machine. The final results appear in Table 5.

Table 5. Example of final results file. Antiproton dipoles data.

NAME	TYPE	X(INCHES)	Y (INCHES)	Z (INCHES)	PITCH (MR)	ROLL (MR)
A1B07	SDB-004 UP	-4563.210	-15379.824	100.730	-0.1537602	-0.9345022
A1B07	SDB-004 CT	-4528.013	-15331.626	100.721		
A1B07	SDB-004 DN	-4486.640	-15288.613	100.712		
A1B08	SDA-002 UP	-4425.475	-15227.387	100.722	-0.0381277	-0.6284594
A1B08	SDA-002 CT	-4358.924	-15167.063	100.718		
A1B08	SDA-002 DN	-4283.477	-15118.321	100.715		
A1B09	LDA-004 UP	-4208.817	-15075.224	100.690	0.1038372	-0.7356417
A1B09	LDA-004 CT	-4128.745	-15034.093	100.699		
A1B09	LDA-004 DN	-4043.059	-15006.500	100.708		
A1B10	LDA-012 UP	-3987.009	-14991.310	100.757	0.1996040	-1.0442187
A1B10	LDA-012 CT	-3898.977	-14972.478	100.774		
A1B10	LDA-012 DN	-3809.056	-14968.182	100.792		
A2B10	LDA-001 UP	-2741.848	-14967.974	100.742	-0.2801255	0.3239970
A2B10	LDA-001 CT	-2651.892	-14972.378	100.717		
A2B10	LDA-001 DN	-2563.843	-14991.325	100.692		
A2B09	LDA-002 UP	-2507.884	-15006.321	100.731	-0.2780792	-0.6703490
A2B09	LDA-002 CT	-2422.157	-15033.918	100.706		
A2B09	LDA-002 DN	-2342.047	-15075.063	100.681		
A2B08	SDA-001 UP	-2267.499	-15118.139	100.746	-0.2654553	-1.0733267
A2B08	SDA-001 CT	-2192.016	-15166.825	100.722		
A2B08	SDA-001 DN	-2125.419	-15227.099	100.698		
A2B07	SDB-005 UP	-2064.128	-15288.326	100.735	-0.1830194	-1.1359440
A2B07	SDB-005 CT	-2022.773	-15331.369	100.724		
A2B07	SDB-005 DN	-1987.597	-15379.596	100.714		
A3B03	SDC-003 UP	-803.621	-17230.180	100.838	-0.1479707	-1.3234902
A3B03	SDC-003 CT	-788.219	-17255.338	100.833		
A3B03	SDC-003 DN	-776.507	-17282.411	100.829		
A3B07	SDB-006 UP	-304.288	-18294.859	100.845	0.1788642	-0.5277130
A3B07	SDB-006 CT	-280.162	-18349.441	100.855		
A3B07	SDB-006 DN	-263.615	-18406.778	100.866		
A3B08	SDA-004 UP	-241.294	-18490.419	100.888	-0.5865359	-0.6481779
A3B08	SDA-004 CT	-222.249	-18578.183	100.835		
A3B08	SDA-004 DN	-217.676	-18667.874	100.783		
A3B09	LDA-005 UP	-217.704	-18754.157	100.865	-0.2015590	-0.8842509
A3B09	LDA-005 CT	-222.169	-18844.075	100.847		
A3B09	LDA-005 DN	-241.166	-18932.076	100.829		
A3B10	LDA-003 UP	-256.317	-18987.999	100.861	0.0080813	-1.2763688
A3B10	LDA-003 CT	-283.792	-19073.765	100.862		
A3B10	LDA-003 DN	-324.823	-19153.934	100.863		
A4B10	LDA-007 UP	-858.688	-20078.059	100.904	-0.1222459	-1.3156916
A4B10	LDA-007 CT	-907.334	-20153.789	100.893		

5. References of magnets

Another application of the laser tracker used by the Metrology and Alignment group is the remote referencing of the magnetic components of the quadrapole and dipole magnets prior to installation in the beam lines. The reference survey or fiducialization of these magnets obtain (X, Y, Z) Cartesian coordinates on selected fiducials mounted externally on the magnet with respect to the magnets "sweet spot."

1. Some referencing occurs "on the table" where fiducial points are located in respect to geometrical center of the magnet. In this reference process all points must be transformed to coordinates as showed on Figure 6.
   A reference coordinate system is created by the intersection of mid planes from the top and bottom, left and right, and upstream and downstream planes with the condition of perpendicularity. The coordinate of each point is determined with simple normal distances calculated from each of the mid planes.

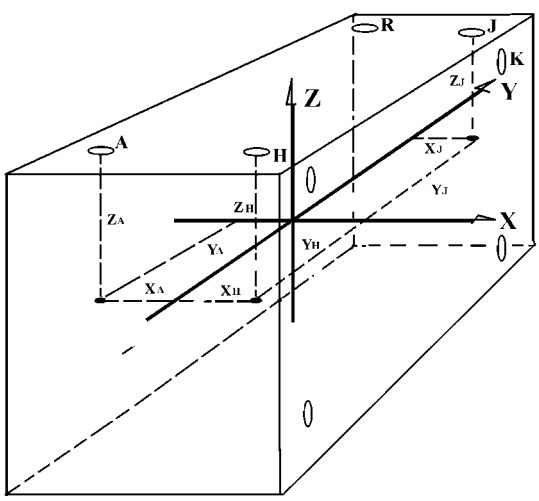

Figure 6. Reference on the table coordinates system

2. An alternative method is to use a stretch wire reference table (Figure 7). In this scenario, the magnet factory will have positioned a wire near the magnetic centerline of the magnet.

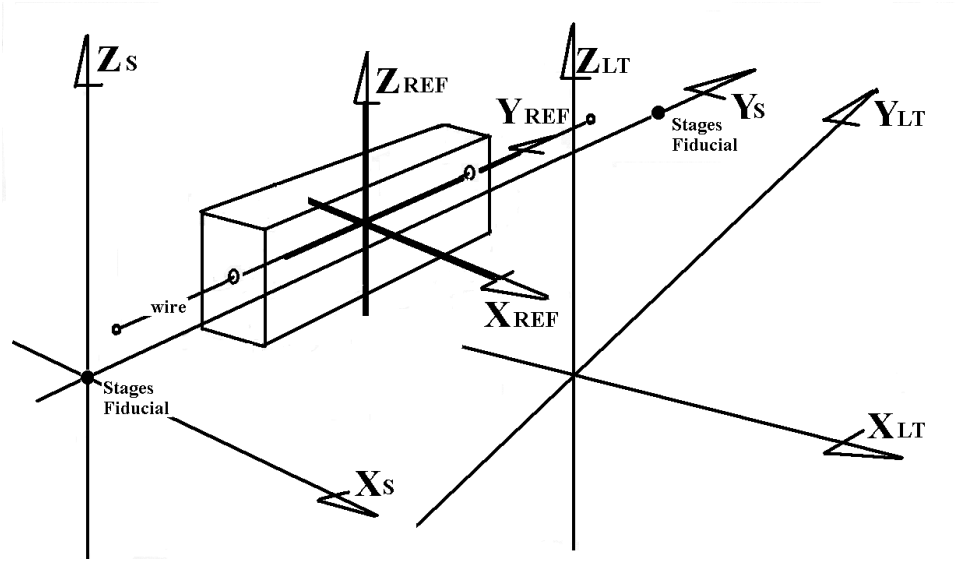

where chain of transformation:

X_{LT} Y_{LT} Z_{LT} - LASER TRACKER Coordinates system, X_S Y_S Z_S - STAGES Coordinates system and X_{REF} Y_{REF} Z_{REF}-MAGNET REFERENCE Coordinates system

Figure 7. Stretch wire reference strategy of coordinates system transformation

The stages on either end of the magnet, secure the wire, and are adjusted so as to move the wire to the magnets centerline. The relationship between fixed reference points on the stages and the points of attachment are known. Measurements are made to the reference points and the fiducials installed on the magnets. A right hand reference coordinate system is created with the Y Z plane passing through the points where wire is attached to the stages, the Z-axis is a gravity vector and the X-axis is an orthogonal vector to Y and Z plane with the origin at the magnetic center of the magnet. The center of the magnet is either determined with the half-length of the magnet or the center punch mark established by the magnet factory.

6. Acknowledgments

We express our thanks to Mr. John Kyle and Mr. Charles Wilson for their diligent field survey and assistance in the preparation of the data upon which this paper is based.

References

[1] Babatunde Oshinowo, *Error Propagation for Laser Tracker Distances* unpublished information,1996

[2] Dijak E. *"Challenges in cost cutting Fixtures design "* Proceedings of the 5th International Workshops on Accelerator Alignment, Argonne National Laboratory, October 14-17, 1997

[3] Gracie, G., Mikhail, E. M. *Analysis and Adjustment of Survey Measurements*, New York: Van Nostrand Reinhold Company Inc., 1981

[4] Martusewicz , J. *Positional transformation*, Warsaw: Geodezja i Kartografia t. XLIX, Z. 3, S, 123 – 129 (2000)

[5] Urho A Uotila, *Notes on Adjustment and Computations Part* I, Department of Geodetic Science and Surveying The Ohio State University, 1986

[6] Wojcik G. J., Lakanen S. A. *"The Adjustment of the Fermilab Main Injector Underground Geodetic Survey"* Proceedings of the 5th International Workshops on Accelerator Alignment, Argonne National Laboratory, October 14-17, 1997

[7] Wojcik G. J., Lakanen S. A. "The Survey of antiproton Accumulator Ring at Fermilab Proceedings of the 5th International Workshops on Accelerator Alignment, Argonne National Laboratory, October 14-17, 1997

[8] Wojcik G.J., Kyle J, Wilson C, "*Low Beta Quads creation magnet coordinates system"* unpublished information, January 2000

Appendix A

```
PROGRAM CHABA
*************************************************************************
*                                                                       *
*     FILE 52.OUT                                                       *
*                                                                       *
*************************************************************************

   REJECTION TOLERANCE FOR THE ACTIVE POINTS    1.00000

   TRANSFORMATION DATA   Xnew = S * Ry * Rx * Rz * Xold + Xo
   ************************************************************************
   *TERMS OF ROTATION MATRIX (Phi,Omega,Kappa)                            *
   *  P1  =   0.9999999938  P2  =   0.0000362497  P3  =   0.0001053518   *
   *  Q1  =  -0.0000362537  Q2  =   0.9999999986  Q3  =   0.0000375857   *
   *  R1  =  -0.0001053505  R2  =  -0.0000375895  R3  =   0.9999999937   *
   *          ANGLES OF ROTATION                                         *
   *  KAPPA (Z AXIS) =   399.997692018  (ESTIMATED)                      *
   *  OMEGA (X AXIS) =     0.002392779  (ESTIMATED)                      *
   *  PHI   (Y AXIS) =   399.993293095  (ESTIMATED)                      *
   *          SCALE FACTOR                                               *
   *  Sxyz =    0.9999996272  (ESTIMATED)                                *
   *          TRANSLATION VECTOR                                         *
   *  Xo  =   0.030667 (EST) Yo  =  0.017833 (EST) Zo  = -0.429167 (EST) *
   ************************************************************************

                      COORDINATES OF ACTIVE POINTS

                   NEW      SYSTEM                      OLD     SYSTEM
NOM     X(inches)   Y(inches)   Z(inches)  X(inches)    Y(inches)   Z(inches)
PP109  -4790.394   -15698.441   116.602   -4790.441   -15698.444   117.08500
PP111  -5063.976   -16065.533   102.945   -5064.008   -16065.546   103.39300
PP112  -5169.316   -15951.596   116.607   -5169.353   -15951.614   117.04800
PP113  -5260.117   -16131.215   107.551   -5260.147   -16131.237   107.96800
PP116  -5442.166   -16425.160   116.635   -5442.186   -16425.189   117.02300
PP117  -5348.065   -16505.654   102.870   -5348.083   -16505.676   103.26800

  ADJUSTED COORDINATES OF ACTIVE POINTS FROM OLD SYSTEM TO NEW SYSTEM

NOM     X(inches)   Y(inches)  Z(inches) DX(mils) DY(mils) DZ(mils) DD(mils))
PP109  -4790.394   -15698.440   116.599  -0.21      0.81     -3.32      3.42
PP111  -5063.976   -16065.533   102.949   0.15      0.35      4.31      4.33
PP112  -5169.315   -15951.596   116.611   0.76     -0.36      4.12      4.20
PP113  -5260.117   -16131.216   107.547   0.32     -1.34     -3.56      3.82
PP116  -5442.165   -16425.161   116.633   0.69     -1.29     -2.34      2.76
PP117  -5348.067   -16505.652   102.871  -1.71      1.81      0.78      2.61

           ***  EMQ DD = 3.58 mils  ***

  COORDINATES OF PASSIVE POINTS IN NEW SYSTEM

 NOM           X(inches)     Y(inches)      Z(inches)
 1            -5338.832     -16510.838      114.111
 2            -5334.074     -16502.594      114.110
 3            -5328.682     -16493.264      114.104
 1            -5330.249     -16495.949       87.540
 2            -5333.535     -16501.644       87.541
 3            -5337.540     -16508.574       87.543
 1            -5329.623     -16516.917      117.447
 2            -5319.459     -16499.923      117.431
A1Q01U        -5337.956     -16514.138      117.093
```

Input files for Helmert transformation (transformation from no gravity to gravity system)

FILE 52.OLD Coordinates in no gravity system			
(A6,3(F15.7))			
PP109	-4790.441	-15698.444	117.085
PP111	-5064.008	-16065.546	103.393
PP112	-5169.353	-15951.614	117.048
PP113	-5260.147	-16131.237	107.968
PP116	-5442.186	-16425.189	117.023
PP117	-5348.083	-16505.676	103.268
1	-5338.849	-16510.862	114.509
2	-5334.092	-16502.618	114.509
3	-5328.700	-16493.288	114.504
1	-5330.264	-16495.972	87.940
2	-5333.550	-16501.667	87.940
3	-5337.555	-16508.597	87.942
1	-5329.641	-16516.941	117.846
2	-5319.477	-16499.946	117.832
A1Q01	-5337.975	-16514.162	117.491
FILE 52.NEW Coordinates in gravity system			
(A6,3(F15.7))			
PP109	-4790.394	-15698.441	116.602
PP111	-5063.976	-16065.533	102.945
PP112	-5169.316	-15951.596	116.607
PP113	-5260.117	-16131.215	107.551
PP116	-5442.166	-16425.16	116.635
PP117	-5348.065	-16505.654	102.87